IOP Conf. Series: Journal of Physics: Conf. Series **1071** (2018) 012007 doi:10.1088/1742-6596/1071/1/012007

Weak measurement and weak values — New insights and effects in reflectivity and scattering processes

C Aris Chatzidimitriou-Dreismann

Institute of Chemistry, Sekr. C2, Faculty II, Technical University of Berlin, D-10623 Berlin, Germany

E-mail: dreismann@chem.tu-berlin.de

Abstract. Recently, the notions of Weak Measurement (WM), Weak Value (WV) and Two-State-Vector Formalism (TSVF), firstly introduced by Aharonov and collaborators, have extended the theoretical frame of standard quantum mechanics, thus providing a quantum-theoretical formalism for extracting new information from a system in the limit of small disturbance to its state. Here we provide an application to the case of two-body scattering with one body weakly interacting with its environment — e.g. a neutron being scattered from a H_2 molecule physisorbed in a carbon nanotube. In particular, we make contact with the field of incoherent inelastic neutron scattering from condensed systems. We provide a physically compelling prediction of a new quantum effect — a momentum transfer deficit; or equivalently, an enhanced energy transfer; or an apparent reduction of the mass of the struck particle. E.g., when a neutron collides with a H_2 molecule in a C-nanotube and excites its translational motion along the nanotube, it apparently exchanges energy and momentum with a fictitious particle with mass of 0.64 atomic mass units. Experimental results are shown and discussed in the new theoretical frame. The effect under consideration has no conventional interpretation, thus also supporting the novelty of the quantum theoretical framework of WV and TVSF. Some speculative remarks about possible applications being of technological interest (fuel cells and hydrogen storage; Li^+ batteries; information and communication technology) are shortly mentioned.

1. Introduction

The fundamental t-inversion symmetry of the Schrödinger equation plays a crucial role in the novel theory of weak measurement (WM), weak values (WV) and the two-state vector formalism (TSVF) of Aharonov and collaborators [1, 2, 3, 4, 5, 6, 7]. Based on this theory, new experiments were suggested and several novel quantum effects were discovered; see the cited references.

Very recently, Aharonov et al. [8] provided a remarkably simple and clear example demonstrating the predictive power of the theory, revealing an "anomalous" momentum exchange between photons (or particles) passing through a Mach-Zehnder interferometer (MZI) and one of its mirrors. Here the measured photon's (particle's) final state, being post-selected in a specific output of the MZI, plays a crucial and succinct role, together with the basic t-inversion symmetry of quantum mechanics, as captured by the Aharonov-Bergmann-Lebowitz rule [9]. In essence, the revealed effect (which has no conventional interpretation) is as follows: Although the photons (particles) collide with the considered mirror only from the inside of the MZI, they do not push the mirror outwards, but rather they somehow succeed to pull it in [8]; see Sec. 2.

Inspired by this remarkable theoretical result, we recently proposed an application of the theory under consideration, in the context of incoherent inelastic neutron scattering off atoms and/or molecules in condensed matter [10]. Related experimental results obtained by incoherent inelastic neutron scattering (IINS, or INS) and deep-inelastic neutron scattering (DINS) — also called neutron Compton scattering (NCS) — were presented and discussed [10].

In this paper, after a short introduction to the new theory and the aforementioned "anomalous" momentum transfer in a MZI, we present the specification of the theoretical frame to real scattering experiments. In particular, we discuss a counter-intuitive experimental result of neutron scattering from H_2 in carbon nanotubes and related materials, as obtained with conventional INS as well as modern 2-*dimensional* neutron spectrometers, e.g. ARCS [11]. Additionally, an "anomalous" DINS result from H of a solid polymer is presented. In short, our findings correspond to a striking strong *mass deficit* of the scattering objects. These observations have no known conventional interpretation.

The experimental findings and their theoretical interpretation support the view that the quantum theory of WM, WV and TSVF sheds new light on interpretational issues concerning fundamental quantum theory. Moreover, this t-symmetric theoretical formalism offers a new guide for our intuition to design new experiments and discover novel quantum effects.

2. Motivation—A recent theoretical result of quantum optics

The experimental context of this paper concerns
(a) the measurements of *momentum* and *energy* transfer in real scattering experiments,
(b) the predictions of conventional (classical or quantum) theory and
(c) comparison of the experimental results with a new prediction based on the formalism of WM and TSVF.
The latter point may be best motivated by referring directly to some of the intriguing results presented in a recent theoretical paper by Aharonor et al. [8].

Let us first refer to a surprising theoretical prediction derived by Aharonov et al. in Ref. [8]. Here we consider one specific result of this work only, which concerns "anomalous" momentum transfer between two quantum objects (i.e. a photon and a mirror) and thus appears to be in intimate connection with the neutron-atom collision (or scattering) experiments considered in the following sections.

The schematic representation of the experimental setup is shown in Fig. 1.

A photon (or particle) beam enters a device similar to a usual Mach-Zehnder interferometer (MZI), with the exception that one reflecting mirror is sufficiently small (say, a meso- or nanoscopic object M) in order that its momentum distribution may be detectable by a suitable non-demolition measurement [12]. In Ref. [8] the authors show the following astonishing result. Although the post-selected photons (as all photons do, of course) collide with the mirror M only from the *inside* of the MZI, they do not push M outwards, but rather they somehow succeed to *pull it in*. It is obvious that this result cannot have any conventional theoretical interpretation.

Let us now consider a straightforward derivation of this effect, following the presentation of some derivations (relevant to our purposes) of Ref. [8] closely.

The two identical beam splitters of MZI have nonequal reflectivity r and transmissivity t (both real, with $r^2 + t^2 = 1$), say $r > t$. Now we are interested in the momentum kicks given to the mirror M due to the photon-M collisions inside the interferometer, but especially for photons emerging toward detector D_2 in Fig. 1). This corresponds to a post-selection condition. (The effect of the photons emerging toward the other detector, D_1, is of less relevance here.)

Using the standard convention, an incoming state $|\text{in}\rangle$ impinging on the beam splitter will emerge as a superposition of a reflected state $|R\rangle$ and a transmitted state $|T\rangle$; $|\text{in}\rangle \rightarrow ir|R\rangle + t|T\rangle$. Hence when a single photon impinges from the left on BS_1, as illustrated in Fig. 1, the effect of

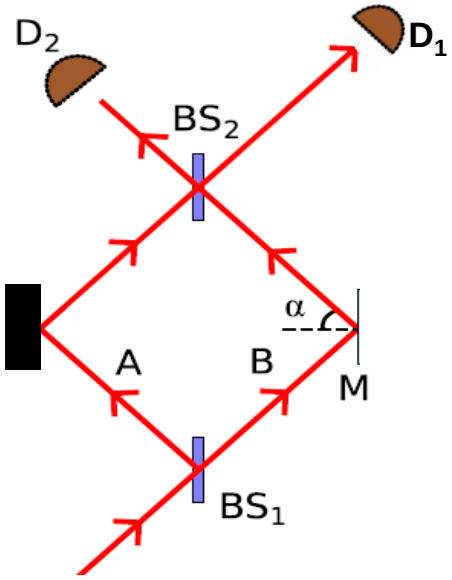

Figure 1. Mach-Zehnder interferometer and path of a light beam (or a particle, etc.). The mirror M in the rhs is a mesoscopic *quantum* object. Of particular interest are the photons (particles) emerging toward detector D_2. (Adapted from Fig. 2 of [8].)

the beam splitter is to produce inside the interferometer the state

$$|\Psi\rangle = ir|A\rangle + t|B\rangle \tag{1}$$

where $|A\rangle$ and $|B\rangle$ denote the photon propagating along the A and B arms of the interferometer, respectively.

The second beamsplitter, BS_2, is identical to the first. As one can readily check, a photon in the quantum state $|\Phi_1\rangle = t|A\rangle - ir|B\rangle$ impinging on the second beamsplitter, emerges towards detector D_1 while a photon in the orthogonal state $|\Phi_2\rangle = -ir|A\rangle + t|B\rangle$ emerges towards detector D_2.

Thus, when a single photon (particle) enters the interferometer by impinging on the left side of the beamsplitter BS_1, the probabilities to be found in the arms A and B are r^2 and t^2 respectively. The probability of emerging towards detector D_1 is $|\langle\Phi_1|\Psi\rangle|^2 = 4r^2t^2$ while the probability of emerging towards D_2 is $|\langle\Phi_2|\Psi\rangle|^2 = (r^2 - t^2)^2 = 1 - 4r^2t^2$.

Firstly, we send a *classical* light (particle) beam of intensity I towards this interferometer. The light (particle) intensity in arm A is then $I_A = r^2I$ while the intensity in arm B is $I_B = t^2I$. The intensities of the output beams, toward the tow detectors, are $I_{D_1} = 4r^2t^2I$ and $I_{D_2} = (1-4r^2t^2)I$. The momentum given to the mirror M by the beam inside the interferometer is $2I_B \cos\alpha = 2t^2I\cos\alpha$. Clearly, this pushes the mirror M outward.

Secondly, let us now send a *quantum* beam of photons (or particles) into the MZI. Each photon incident on M gives it a momentum kick δ. Note that each individual momentum kick must be much smaller than the spread Δ of momentum of the mirror M. This is a general property of any interferometer. It has to be so in order to maintain the coherence of the beam in the interferometer; otherwise the photons (particles) will become entangled with the mirror

IOP Conf. Series: Journal of Physics: Conf. Series **1071** (2018) 012007 doi:10.1088/1742-6596/1071/1/012007

M. To show this, we note that a photon when going through arm A will produce no kick to M while when going through arm B it will. Accordingly, if $\phi(p)$ is the initial quantum state of M and by $|\Psi\rangle$ the quantum state of the photon after the input beam splitter BS_1, but before reaching the mirror, the reflection on the mirror results in

$$|\Psi\rangle\phi(p) = (ir|A\rangle + t|B\rangle)\phi(p) \to ir|A\rangle\phi(p) + t|B\rangle\phi(p-\delta) \tag{2}$$

If $\phi(p)$ is orthogonal to $\phi(p-\delta)$ where δ is the kick given by the photon, then the photon ends up entangled with the mirror and coherence is lost. Another way of looking at this is to note that the mirror has to be localized within a distance smaller than the wavelength of light, otherwise there will be phase fluctuations larger than 2π and interference is lost.

[In fact the spread Δ in the momentum of the mirror has to be many times bigger — of order $\sqrt{\overline{n}}$ times - than that of an individual kick to ensure coherence when a beam with an average of $\overline{n}$ photons and a spread $\sqrt{\overline{n}}$ goes through the interferometer. At the same time Δ, being of order $\sqrt{\overline{n}}\delta$, is small enough so that the average kick, which is of order $\overline{n}\delta$ is detectable.]

For simplicity we take the state of the mirror to be (up to normalisation) $\phi(p) = \exp(-\frac{p^2}{2\Delta^2})$. Consider now a single photon propagating through the interferometer. Given that $\delta \ll \Delta$, we can approximate the state (2) of the photon and mirror just before the photon reaches the output beamsplitter by

$$\begin{aligned} |\Psi\rangle\phi(p) &\approx ir|A\rangle\phi(p) + t|B\rangle\Big(\phi(p) - \frac{d\phi(p)}{dp}\delta\Big) \\ &= |\Psi\rangle\phi(p) - t|B\rangle\frac{d\phi(p)}{dp}\delta \end{aligned} \tag{3}$$

Suppose now that the photon emerges in the beam directed towards detector D_2. The state of the mirror M is then given (up to normalization) by projecting the joint state onto the state of the photon corresponding to this beam, i.e.

$$\begin{aligned} & \langle\Phi_2|\Big(|\Psi\rangle\phi(p) - t|B\rangle\frac{d\phi(p)}{dp}\delta\Big) \\ = \;& \langle\Phi_2|\Psi\rangle\Big(\phi(p) - \frac{t\langle\Phi_2|B\rangle}{\langle\Phi_2|\Psi\rangle}\frac{d\phi(p)}{dp}\delta\Big) \\ = \;& \langle\Phi_2|\Psi\rangle\Big(\phi(p) - \frac{\langle\Phi_2|\mathbf{P}_B|\Psi\rangle}{\langle\Phi_2|\Psi\rangle}\frac{d\phi(p)}{dp}\delta\Big) \\ = \;& \langle\Phi_2|\Psi\rangle\phi(p - P_B^w\delta) \end{aligned} \tag{4}$$

Here $\mathbf{P}_B = |B\rangle\langle B|$ is the *projection operator* on state $|B\rangle$ and

$$P_B^w = \frac{\langle\Phi_2|\mathbf{P}_B|\Psi\rangle}{\langle\Phi_2|\Psi\rangle}$$

is the so called *weak value* (WV) of $\mathbf{P}_B$ between the initial state $|\Psi\rangle$ and the final state $|\Phi_2\rangle$ [1, 2, 3, 4, 5, 6, 7]. The value of P_B^w is readily found to be

$$\begin{aligned} P_B^w &= \frac{\langle\Phi_2|\mathbf{P}_B|\Psi\rangle}{\langle\Phi_2|\Psi\rangle} = \frac{(ir\langle A| + t\langle B|)\mathbf{P}_B(ir|A\rangle + t|B\rangle)}{(ir\langle A| + t\langle B|)(ir|A\rangle + t|B\rangle)} \\ &= -\frac{t^2}{r^2 - t^2} \end{aligned} \tag{5}$$

Hence the momentum kick received by the mirror due to a photon emerging towards D_2 is

$$\delta p_M = P_B^w \, \delta = -\frac{t^2}{r^2 - t^2} \, \delta \tag{6}$$

The appearance in the above expressions of the WV of the projector $\mathbf{P}_B$ is not accidental. Indeed, we can view the mirror as a measuring device measuring whether or not the photon is in arm B or not. The momentum of the mirror acts as a "pointer" (no kick — the photon is in arm A; kick — the photon is in arm B). However, since the photon can only change the position of the pointer (i.e. the momentum of the mirror) by far less than its spread, we are in the so called "weak measurement" [1, 2, 3, 4, 5, 6, 7] regime.

Finally, the total momentum given to the mirror by all the photons emerging towards D_2 is given by the momentum due to each photon times the number of photons in the beam. Using the fact that the probability of a photon to end in this beam is $(r^2 - t^2)^2$ we obtain

$$\delta p_M = \overline{n}(r^2 - t^2)^2 \frac{-t^2}{r^2 - t^2} \delta = -t^2 \overline{n}(r^2 - t^2) \, \delta < 0 \tag{7}$$

Since we investigated the case with $r > t$, the sign of the momentum received by the mirror is negative, hence the mirror is pushed towards the inside of the MZI. This momentum change is a result of the mirror receiving a *superposition* between a kick δ and no kick at all, corresponding to the photon (particle) propagating through the two MZI-arms.

To summarize: The physical insight obtained from quantum mechanics is dramatically different from the classical one. In fact, according to quantum mechanics, the photons that end up in the D_2 beam give negative momentum kick on M. Astonishingly, although they collide with the mirror only from the inside of the MZI, they do not push the mirror outwards; rather they somehow succeed to pull it in! This is realized by a superposition of giving the mirror zero momentum and positive momentum — the superposition results in the mirror gaining negative momentum.

Concluding the above short discussions, one may say that the new insights and/or predictions made possible within the theoretical frame of WV and TSVF are not limited to interpretational issues only. The revised intuitions can lead one to find novel quantum effects that can be measured in real experiments.

3. On post-selection, weak measurement, weak values and two-state-vector formalism

Weak quantum measurement (WM) is unique in measuring noncommuting operators and revealing new counter-intuitive effects predicted by the two-state-vector-formalism (TSVF) [3, 6]. The main aim of this article is to point out certain new (and experimentally observable) features of elementary scattering processes predicted within the theoretical frame of WM and TSVF, and which contradict every conventional expectation; cf. [10]. Concretely, we have in mind incoherent-inelastic scattering of single (massive) particles, (e.g. neutrons or electrons) from nuclei and/or atoms.

As the starting point of the new theory under consideration one usually considers the paper [2] by Aharonov, Albert and Vaidman, and the earlier paper [9] by Aharonov, Bergmann and Lebowitz. Here some short remarks may be helpful.

A standard von Neumann (also called "strong") measurement yields the eigenvalues of the measured observable, but at the same time disturbs the measured system. According to standard theory [13], the final state of the system after the measurement becomes an eigenstate of the measured observable. This usually changes the initial state of the system. On the other hand, by coupling a measuring device to a system sufficiently weakly, it may be possible to read out

certain information while limiting the disturbance induced by the measurement to the system. As Aharonov and collaborators originally proposed [2, 9], one may achieve new physical insights when one furthermore post-selects on a particular outcome of the experiment. In this case the eigenvalues of the measured observable are no longer the relevant quantities; rather the measuring device consistently indicates the *weak value* (WV) [2, 9] given by

$$A_w \equiv \frac{\langle \psi_f | \hat{A} | \psi_i \rangle}{\langle \psi_f | \psi_i \rangle} \tag{8}$$

where $\hat{A}$ is the operator whose value is being ascertained, $|\psi_i\rangle$ is the initial state of the system, and $|\psi_f\rangle$ is the state that is post-selected (e.g. by performing a specific measurement). Note that the number A_w may be complex.

The significance of this formula is as follows. Let us couple a measuring device whose pointer has position coordinate q to the system $\mathcal{S}$, and subsequently measure its conjugated momentum p. The coupling interaction is taken to be the standard von Neumann measurement interaction [13]

$$\hat{H} = -g\, \hat{q} \otimes \hat{A} \tag{9}$$

The coupling constant g is assumed to be appropriately small and the interaction time sufficiently short. Then the mean value $\langle p \rangle$ of the pointer momentum is given by [2]

$$\langle p \rangle = g\ Re[A_w] \tag{10}$$

where Re denotes the real part. This formula requires the initial pointer momentum wavefunction to be real and centered at $\langle p \rangle = 0$ before measurement, but these assumptions can easily be relaxed; see cited references.

The formula (8) implies that, if the initial state $|\psi_i\rangle$ is an eigenstate of a measurement operator A, then the weak value post-conditioned on that eigenstate is the same as the classical (strong) measurement result. When there is a definite outcome, therefore, strong and weak measurements agree. Interestingly, a WM can yield values outside the range of measurement results predicted by conventional theory [2].

For some experiments, but not in those considered in this paper, a WV can also be complex, with its imaginary part affecting the pointer position. I.e., the mean of the pointer position after measurement is given by

$$\langle q \rangle = 2gv\ Im[A_w] \tag{11}$$

where Im denotes the imaginary part and v is the variance in the initial pointer spatial position [2], with $\langle q \rangle = 0$ before measurement.

The situation we shall consider is where a system $\mathcal{S}$ evolves unitarily from an initial state $|\psi_i\rangle$ to a final post-selected measurement outcome $\langle \psi_f|$. At various time points inbetween, observables may be measured weakly. Here we consider the scenario where there is a single copy of the system, with the measuring device weakly coupled to it.

In the simplest case where there is just one observable A, we assume the evolution from $|\psi_i\rangle$ to the point where A is measured is given by U, and from this point to the post-selection the evolution is given by V. Then we can rewrite (8) as:

$$A_w = \frac{\langle \psi_f | \hat{V} \hat{A} \hat{U} | \psi_i \rangle}{\langle \psi_f | \hat{V} \hat{U} | \psi_i \rangle} \tag{12}$$

and the mean of the pointer is given by (10) as before.

The fact that one only sufficiently "weakly" disturbs the system in making WMs means that one can in principle measure different variables in succession. This theoretical observation has led to a great number of experimental applications and discovery of several new effects; see e.g. [1, 2, 3, 4, 5, 6, 7, 10] and references cited therein.

4. Elementary scattering in view of WV and TSVF

4.1. Momentum transfer in impulsive two-body collisions

In this theoretical section, we present the basic result of WV and TSVF as applied to scattering processes, especially non-relativistic neutron scattering, firstly obtained in Ref. [10].

Here we mainly follow the presentation of that reference.

The position and momentum of the neutron (probe particle) are denoted as (q, p). Similarly, the position and momentum of the scatterer (atom, nucleus) are denoted as (Q, P). $\hat{X}$ may represent the corresponding operator of a physical quantity X. For simplicity, let us consider here a one-dimensional quantum model for momentum exchange in a two-particle impulsive collision.

In the usually considered, but extremely limiting case in which both particles occupy states with well defined momenta (i.e. plane waves), the initial state of the two-body system is standardly assumed as a product (uncorrelated) state

$$\Psi_{in} = \phi_n(p) \otimes \Xi_A(P) \tag{13}$$

(indices n and A refer to neutron and atom, respectively). In a first attempt, an impulsive scattering process may be formally approached by the interaction Hamiltonian

$$\hat{V} = F(t)\,(\hat{q} - \hat{Q}) \tag{14}$$

where the function $F(t)$ represents a non-zero force during a short time interval τ, the duration of the collision. We may assume that $F(t)$ is proportional to a delta function. Furthermore, the integral

$$\int_0^\tau F(t)\,dt = \hbar K \tag{15}$$

provides the momentum transfer $\hbar K$ caused by the collision.

Neutron and atom observables commute, so $[\hat{q}, \hat{Q}] = 0$, and the associated unitary evolution operator is

$$\hat{U}(\tau) = e^{-(\imath/\hbar)\int \hat{V} dt} = e^{-(\imath/\hbar)\,\hbar K\,(\hat{q}-\hat{Q})} \equiv e^{-\imath\,K\,\hat{q}} e^{+\imath\,K\,\hat{Q}} \tag{16}$$

The *shift operator* $e^{\imath\hbar K\,\hat{Q}/\hbar}$ describes the momentum shift of an atomic momentum eigenket as $e^{\imath\hbar K\,\hat{Q}/\hbar}|P\rangle = |P + \hbar K\rangle$ while the operator $e^{-\imath\hbar K\,\hat{q}/\hbar}$ shifts neutron's momentum eigenket as $e^{-\imath\hbar K\hat{q}/\hbar}|p\rangle = |p - \hbar K\rangle$ of the impinging particle (neutron). Immediately after the momentum exchange, the state of the two-particle system in the momentum representation is

$$\begin{aligned} \Psi_f &= \hat{U}(\tau)\,\phi_n(p) \otimes \Xi_A(P) \\ &= e^{-i\hbar K\,\hat{q}/\hbar}\phi_n(p) \otimes e^{i\hbar K\,\hat{Q}/\hbar}\Xi_A(P) \\ &= \phi_n(p + \hbar K) \otimes \Xi_A(P - \hbar K) \end{aligned} \tag{17}$$

which is a not entangled final state, due to the trivial form of $\hat{V}$. These introductory considerations may motivate the search for a more appropiate (i.e. more realistic) two-body impulsive interaction Hamiltonian, which is presented in the following section.

4.2. WM, weak interaction Hamiltonian and momentum transfer

Let us now assume that the struck atom is initially at rest. For simplicity of notation, it is sufficient to consider the atomic momentum component parallel to **K**, which from now on we shall denote simply by P—and the associated operator simply by $\hat{P}$. In other words, we consider a one-dimensional problem.

For illustration and motivation of the derivations presented below, we first provide a heuristic derivation of a von Neumann-type [13] interaction Hamiltonian for momentum transfer. Let us start with a formal one-body model Hamiltonian describing momentum transfer $-\hbar K \equiv +\hbar K_n$ *on the neutron* due to the collision with the atom:

$$\hat{V}_n(t) = \delta(t)\,\hbar K\,\hat{q} \tag{18}$$

The associated evolution operator acting on the space of the neutron

$$\hat{U}_n(\tau) = \exp(-\frac{\imath}{\hbar}\,\hbar K\,\hat{q}) \tag{19}$$

shifts a momentum eigenstate of the impinging particle (neutron) as $e^{-\imath\hbar K\hat{q}/\hbar}|p\rangle = |p - \hbar K\rangle$.

Due to momentum conservation in the two-body collision, one has

$$-\hbar K_n = \hbar K_A \equiv \hbar K \tag{20}$$

where $\hbar K_A$ is the momentum transfer *on the atom* due to the collision. (We choose K_A as positive, following standard notation; see e.g. the textbook [14] or the review article [15].)

Let the scattering atom be at rest before collision, $\langle\hat{P}\rangle_i = 0$. Hence, after the collision, it holds

$$\hbar K_A = +\hbar K = \langle\hat{P}\rangle_f = \langle\hat{P}\rangle_f - \langle\hat{P}\rangle_i \tag{21}$$

and correspondingly for the neutron momentum

$$\hbar K_n = -\hbar K = \langle\hat{p}\rangle_f - \langle\hat{p}\rangle_i \tag{22}$$

Hence, the aforementioned operator $\hat{U}_n(\tau)$ of the neutron, Eq. (19), may be written as

$$\hat{U}_n(\tau) = \exp(-\frac{\imath}{\hbar}\,\langle\hat{P}\rangle_f\,\hat{q}) \tag{23}$$

To apply the theory of weak measurement (WM) and two-state-vector formalism (TSVF), a *von Neumann* two-body interaction Hamiltonian is needed; see the associated references cited in the Introduction. Thus one is guided to search of a two-body generalization of the one-body evolution operator $\hat{U}_n(\tau)$ of the form

$$\hat{U}(\tau) = \exp(-\frac{\imath}{\hbar}\,\hat{q}\,\hat{P}) \tag{24}$$

However, this heuristically derived expression still has no direct context to the *realistic* experimental situations under consideration (see Sec. 6 below). To achieve this, we now may proceed as follows.

To begin with, let us refer to the so-called *impulse approximation* (IA) of standard theory [15, 22, 21] and Eq. (38) regarding energy conservation (see Sec. 5):

$$E = \frac{(\hbar K)^2}{2M} + \frac{\hbar\mathbf{K}\cdot\mathbf{P}}{M}$$

Looking at this equation, and having the WV and TSVF in mind, one sees that the *larger* recoil term $\frac{(\hbar K)^2}{2M}$ may be viewed to result from a *strong* impulsive interaction (associated with momentum transfer $+\hbar K$ on the atom). The theoretical treatment of this part of the interaction can be found in standard textbooks (e.g. [14]) but is not within the scope of the present paper. Since in the impulse approximation (IA) holds $|K| \gg |P|$, the *smaller* Doppler term $\frac{\hbar\mathbf{K}\cdot\mathbf{P}}{M}$

may correspond to a *weaker* interaction, in which the atomic momentum $\hat{P}$ couples with an appropriate dynamical variable of the neutron, say $\hat{\mathcal{O}}_n$. Looking at the preceding formulas (23,24) for the model operator effectuating momentum transfer, it appears that this dynamical variable should be $\hat{q}$, that is $\hat{\mathcal{O}}_n = \hat{q}$.

In view of the theory of WV and TSVF, the weak interaction is expected to cause weak *deviations* from the conventionally expected *large* momentum transfer $\hbar K$. This can be formally captured by replacing $\hat{P}$ with the *small* momentum difference $\hat{P} - \hbar K \hat{I}_A$, and also including a positive *smallness* factor

$$0 < \lambda \ll 1$$

in the model interaction Hamiltonian. Summarizing these considerations, let us assume the model interaction Hamiltonian

$$\hat{H}_{int}(t) = +\lambda\, \delta(t)\, \hat{q} \otimes (\hat{P} - \hbar K\, \hat{I}_A) \tag{25}$$

It should be pointed out that the *plus sign* in front of this expression is *not* arbitrary, since it is consistent with the aforementioned definitions (20) of momentum transfer. This point plays a decisive role in the context of the new quantum effect of momentum transfer deficit.

For further physical motivation of the two parts of the model Hamiltonian of Eq. (25), it may be helpful to compare the above reasoning with an example by Aharonov et al. [16], p. 3:

"Consider, for example, an ensemble of electrons hitting a nucleus in a particle collider. [...] Their initial states are known, and a specific post-selection is done after the interaction. The main interaction is purely electromagnetic, but there is also a relativistic and spin-orbit correction in higher orders which can be manifested now in the form of a weak interaction."

4.3. WV of atomic momentum operator $\hat{P}$ and the effect of "anomalous" momentum transfer
Here, the atom represents the system of the general formalism. Since the WV of the identity operator is $(\hat{I}_A)_w = 1$, for the WV of the atomic coupling operator $\hat{P} - \hbar K\, \hat{I}_A$ in the above interaction Hamiltonian holds:

$$(\hat{P} - \hbar K\, \hat{I}_A)_w = P_w - \hbar K \tag{26}$$

To proceed, we first calculate the WV P_w of $\hat{P}$ for some characteristic (and experimentally relevant) final state in momentum space. The derivation is rather straightforward and reveals a striking deviation — more precisely, a deficit — from the conventionally expected momentum transfer to the neutron. The latter represents the pointer of general theory, and the pointer momentum variable $\hat{p}$ is conjugated to $\hat{q}$ contained in Eq. (25).

Moreover, for the calculation of the WV, it is natural to use the momentum space representation, as scattering experiments usually measure momenta (rather than the positions of the scatterers in real space).

Let the atom initially be in a spatially confined state and at rest; e.g. in a potential representing physisorption on a surface; cf. examples in experimental section below. Usually, the initial atomic wave function $\Xi(P)_i$ is approximated by a Gaussian G_A centered at zero momentum,

$$\Xi(P)_i \approx G_A(P).$$

At sufficiently deep temperature the atom will be in its ground state, and the width of $\Xi(P)_i$ is determined by the quantum uncertainty.

It follows that the struck atom moves in the direction of momentum transfer $\hbar K_A = \hbar K$; therefore, to simplify notations, in the following calculations P represents the atomic momentum along the momentum transfer direction.

To be specific, as well as to facilitate the derivations, let us make the following simplifying assumption concerning the final atomic state:

- The final atomic state has the same width in momentum space as the initial state.

However, it may be noted that this assumption is very common in molecular (optical) spectroscopy. It captures the viewpoint that the impulsive transition is very fast and so the atomic environment didn't have sufficient time to change configuation and adapt to the "disturbance" due to the atomic final state.

In other words, let the final atomic state have the same shape as the initial state, but its center should be shifted from zero to the transferred momentum, i.e.

$$\Xi(P)_f = \Xi(P - \hbar K_A)_i. \tag{27}$$

The WV of the atomic momentum operator $\hat{P}$ is calculated as follows:

$$\begin{aligned} P_w &= \frac{\langle \Xi_f | \hat{P} | \Xi_i \rangle}{\langle \Xi_f | \Xi_i \rangle} \\ &= \frac{\int dP\, \Xi(P - \hbar K_A)_i\, P \Xi(P)_i}{\int dP\, \Xi(P - \hbar K_A)_i\, \Xi(P)_i} \\ &= +\frac{\hbar K_A}{2} \\ &= +\frac{\hbar K}{2} \end{aligned} \tag{28}$$

The last equality follows immediately from (a) the two symmetrically distributed Ξ functions around their central position $\bar{P} = \hbar K_A/2$ and (b) the linear term P in the integral of the nominator.

It should be noted that this result does not depend on the width of Ξ, as long as the two Ξ functions are not orthogonal to each other.

Thus we arrived at the following striking conclusion: The momentum transfer comes out to be only half of the conventionally expected value $\hbar K$.

This is a quite interesting result because it represents a momentum-transfer deficit of 50%; i.e. the scattered neutron measures a momentum kick being only half of the conventionally expected value. In more detail, it holds

$$(\hat{P} - \hbar K\, \hat{I}_A)_w = +\frac{\hbar K_A}{2} - \hbar K = -\frac{\hbar K}{2} \tag{29}$$

To proceed, one should note the change of sign between the usually applied interaction Hamiltonian of Eq. (9), as e.g. treated in [2], and the presently used specific form (25). Therefore, there is a corresponding change of sign in Eq. (10),

$$\langle \hat{p} \rangle_f - \langle \hat{p} \rangle_i = -g\, \mathrm{Re}[A_w] \tag{30}$$

Thus one obtains for the *correction* to the shift of the meter pointer variable:

$$\langle \hat{p} \rangle_f - \langle \hat{p} \rangle_i = -\lambda\, (\hat{P} - \hbar K\, \hat{I}_A)_w = +\lambda\, \frac{\hbar K}{2} \tag{31}$$

Moreover, for the *total* momentum transfer shown by the pointer of the measuring device (here: of neutrons) we have

$$\begin{aligned} [\langle \hat{p} \rangle_f - \langle \hat{p} \rangle_i]_{\text{total}} &= [\langle \hat{p} \rangle_f - \langle \hat{p} \rangle_i]_{\text{conventional}} \\ &\qquad + [\langle \hat{p} \rangle_f - \langle \hat{p} \rangle_i]_{\text{correction}} \\ &= -\hbar K + \lambda\, \frac{\hbar K_A}{2} \end{aligned} \tag{32}$$

This expression represents the new quantum effect of *momentum-transfer deficit*: the absolute value of momentum transfer on the neutron predicted by the new theory is *smaller* than that predicted by conventional theory:

$$|-\hbar K + \lambda\,\hbar K_A/2| \leq |-\hbar K| \tag{33}$$

Recall that by definition holds $\hbar K_A = \hbar K$; see Eq. (20).

4.3.1. Plane waves — The limiting case of conventional momentum transfer. Moreover, it is interesting to point out the succinct reason of this large "anomaly" by the following calculation. Let us now make the usual assumption of conventional theory (see e.g. [14, 15, 22]) which is:

- The final state should be a plane wave (i.e. it has vanishing width in momentum space) — as assumed in general conventional theory and the IA.

Here we will show straightforwardly that the result of conventional theory is reproduced.

Namely, now the final state is a delta function (in momentum space), that is, the momentum wave function is a delta function δ_A centered at the assumed transferred momentum $\hbar K_A$,

$$\Xi(P)_f = \delta_A(P - \hbar K_A). \tag{34}$$

The weak value of $\hat{P}$ follows straightforward:

$$\begin{aligned} P_w &= \frac{\langle \Xi_f | \hat{P} | \Xi_i \rangle}{\langle \Xi_f | \Xi_i \rangle} \\ &= \frac{\int dP\, \delta_A(P - \hbar K_A)\, P\Xi(P)_i}{\int dP\, \delta_A(P - \hbar K_A)\, \Xi(P)_i} \\ &= \frac{\hbar K_A\, \Xi(\hbar K_A)_i}{\Xi(\hbar K_A)_i} \\ &= +\hbar K_A \equiv +\hbar K \end{aligned} \tag{35}$$

(Recall the notations of Eq. (20).) Hence, the WV of the system coupling operator $(\hat{P} - \hbar K\, \hat{I}_A)$ is just zero,

$$(\hat{P} - \hbar K\, \hat{I}_A)_w = P_w - \hbar K = 0 \tag{36}$$

[According to standard quantum scattering theory, the scattered wave may acquire an additional phase factor, say $e^{i\chi}$, which does not affect the preceding result because this factor cancels out in the fractions of Eqs. (35).]

This physically means that, under the usual assumption of "plane waves", the new theory yields *no correction* to the conventionally expected value of momentum transfer:

$$\langle \hat{p} \rangle_f - \langle \hat{p} \rangle_i = -\lambda\, (\hat{P} - \hbar K\, \hat{I}_A)_w = 0 \tag{37}$$

And hence the pointer of the measuring device will show the conventionally expected value $-\hbar K$. Thus, the result of Eq. (36) is consistent with conventional theory of the impulse approximation (IA, see below) and, more generally, of incoherent neutron scattering. Clearly, as the standard result of conventional theory is now reproduced, this is a very satisfactory result.

Comparison of the aforementioned two derivations shows immediately that the degree of the momentum transfer "anomaly" under considerations depends on the "deformation" of the shape of the final atomic state. E.g., if the final state is, say, "nearly" a delta function (plane wave), then the anomalous momentum transfer deficit will be "small" — and perhaps remain undetectable.

The rather *general* scheme of the above derivations provides evidence that the new effect under consideration is of a general character and thus may apply to any field of scattering physics, (perhaps even to relativistic scattering in high-energy physics). The immediate implication is that the general theory of WV and TSVF may be relevant for a broad range of modern scattering experiments.

5. Two-body collision — Momentum- and energy-transfer

In a typical scattering experiment, the involved amounts of energy and momentum transfer are determined. (Angular momentum or spin measurements play no role in this paper.) However, this determination involves not only directly measured quantities, but also several theoretically motivated "beliefs" and/or insights based on some "commonly applied" theory. Let us have a short look at these issues.

Modern neutron spectrometers are time-of-flight (TOF) instruments; cf. Fig. (2). Here, a short pulse of neutrons produced at a spallation source (e.g. SNS or ISIS) reaches the first monitor of the spectrometer which triggers the measurement of TOF. A neutron scatters from the sample and may reache the detector, which stops the TOF measurement.

Note that instrumental details play a crucial role in the theoretical framework under consideration, because they concern pre-selection and, in particular, post-selection being essential for the TSVF. Therefore the following facts should be pointed out.

(a) From the measured TOF-values, but without using the actual value of scattering angle θ, one determines the value of $k_1 = |\mathbf{k}_1|$, and consequently of energy transfer $E = \hbar\omega$; see Eq. 38.

(b) Momentum transfer $\hbar\mathbf{K}$, as defined in Eq. (39), is determined from both the scattering angle θ and the TOF value.

(c) Furthermore, from each TOF-value measured with the detector at θ, the associated transfers of momentum ($\hbar K$) and energy ($E = \hbar\omega$) of the neutron to the struck particle are uniquely determined; see e.g. [10]. Hence a specific detector measures only one specific trajectory in the whole K–E plane. Obviously, this fact is related to the *post-selection* of the WV and TSVF theory under consideration

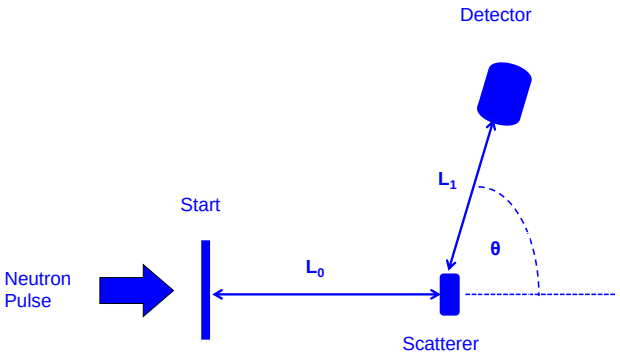

Figure 2. Schematic presentation of a time-of-flight scattering experiment.

In the following sections of this paper, the preceding theoretical considerations and results

are applied to concrete neutron scattering experiments, especially to *incoherent* scattering. In simple terms, "incoherent" means that the impinging neutron (more generally: photon, electron, atom, etc.) collides with, and scatters from, a *single* particle (nucleus, atom, molecule, etc.) As concerns neutron scattering from protons (commonly referred to also as H-atoms), the scattering is mainly incoherent due to the spin-flip mechanism of neutron-proton collision; see e.g. [14]. A clear first-principles explanation of *coherent* versus *incoherent* scattering may be found in Section 3-3 of the well-known Feynman Lectures [17].

Due to scattering, the impinging neutron causes a momentum transfer $\hbar\mathbf{K}$ and an energy transfer E to the atom. For simplicity, in the following we consider isotropic scattering only, which is overwhelmingly dominant in non-relativistic neutron scattering [14]. These quantities are experimentally determined by standard methods; see e.g. Refs. [10, 14, 15, 20, 21].

Due to momentum conservation, it follows that the neutron receives the opposite momentum $-\hbar\mathbf{K}$. The elastic collision of a neutron and a (free) atom with mass M and initial momentum $\mathbf{P}$ results in the neutron's lost energy $E \equiv \hbar\omega$ being transferred to the struck atom:

$$\begin{aligned} E = E_i - E_f = \hbar\omega &= \frac{(\hbar\mathbf{K}+\mathbf{P})^2}{2M} - \frac{P^2}{2M} \\ &= \frac{(\hbar K)^2}{2M} + \frac{\hbar\mathbf{K}\cdot\mathbf{P}}{M} \end{aligned} \tag{38}$$

E_i and E_f are the neutron's initial and final kinetic energy, respectively. This equation represents energy conservation. Furthermore,

$$\hbar\mathbf{K} = \hbar\mathbf{k}_i - \hbar\mathbf{k}_f \tag{39}$$

where $\mathbf{k}_i$ and $\mathbf{k}_f$ are the neutron's initial and final wavevectors, respectively. The absolute value of $\mathbf{K}$ is given by

$$|\mathbf{K}| = K = \sqrt{k_i^2 + k_f^2 - 2k_i k_f \cos\theta} \tag{40}$$

The first term in the right-hand-side (rhs) of Eq. (38) is the so-called recoil energy,

$$E_{rec} = \hbar\omega_{rec} = \frac{(\hbar K)^2}{2M} \tag{41}$$

and represents the kinetic energy of a recoiling atom being initially at rest, i.e. $\langle P\rangle = 0$. Hence one may write

$$\langle E\rangle = \frac{\hbar^2\langle K\rangle^2}{2M} \equiv \bar{E}_{rec} \tag{42}$$

which holds for the E and $\mathbf{K}$ of the peak center. Thus incoherent scattering from (say, a gaseous sample of) such atoms leads to a experimental recoil peak centered at energy transfer $\bar{E}_{rec}$, and exhibiting a width being caused by the term $\hbar\mathbf{K}\cdot\mathbf{P}/M$, which represents the well known effect of *Doppler broadening* — being the second term in the rhs of Eq. (38).

$$E_{Doppler} = \frac{\hbar\mathbf{K}\cdot\mathbf{P}}{M} \equiv \frac{\hbar K P_\parallel}{M} \tag{43}$$

where $P_\parallel$ denotes the atomic-momentum component parallel to $\mathbf{K}$. For *isotropic* systems (gases, liquids, amorphous solids etc., as those considered below) the specific direction determined by $\mathbf{K}$ becomes immaterial, and thus $P_\parallel$ may represent the projection along any direction.

The above simple formulas of this section capture the features of the so-called *Impulse Approximation* (IA) [15, 21, 20, 22].

Relation (41), also called recoil parabola, is nicely illustrated in Fig. 3, which shows experimental data of incoherent inelastic (Compton, DINS) scattering from ^{4}He atoms in the liquid phase; see [18] for details.

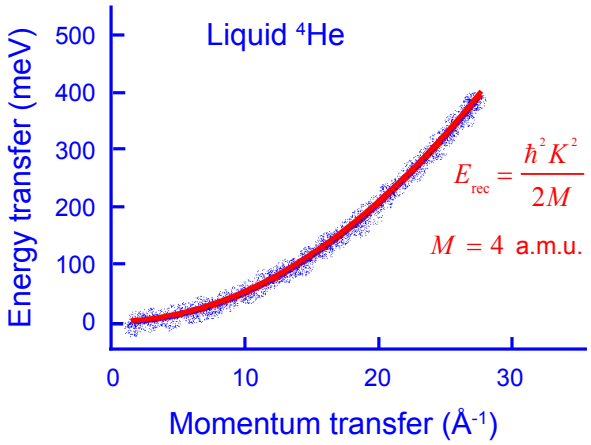

Figure 3. Schematic representation (blue points) of measured dynamic structure factor $S(K, E)$ of liquid helium [18]. The red line is the calculated recoil parabola, according to Eq. (41), for the mass of ^{4}He, shown as a guide to the eye. The white-blue ribbon around the recoil parabola represent data points measured with the time-of-flight spectrometer ARCS [11] (Figure taken from Ref. [10] with permission from Quanta.)

5.1. Effective mass as measured in the scattering experiment

In real experiments, deviations from the impulse approximation are well known; see e.g. [15, 20, 21]. Within conventional theory such deviations are understood as follows.

The energy conservation relation (38) for a two-body collision holds in the so-called impulse approximation, which holds exactly for infinite momentum transfer and, consequently, for quasi-free scattering particles. But it is not completely fulfilled at finite momentum and energy transfers of actual experiments, and thus so-called *final-state effects* (FSE) may become apparent [15, 20, 21]. (In fact, this term commonly includes both *initial and final* state effects). FSE are caused by environmental interactions with the struck particle, which affect both initial and final states of it. Here, we shall shortly discuss this effect in the frame of conventional theory.

Firstly, as Feynman puts it: "We use the term *mass* as a quantitative measure of *inertia* ..." ([19], section 9-1). Therefore, when a scattering particle with mass M is not completely free but *partially bound* to other adjacent particles, then the impinging (or probe, e.g. neutron) particle scatters on an object with *higher* measure of inertia — or higher mass — than M. This is because the adjacent massive particles excert forces on the scattering particle. These forces may be due to some conventional binding mechanisms (such as ionic or van der Waals forces; chemi- or physisorption). However these forces can only hinder the motion of the scattering particle, and thus can never cause an increase of the particle's mobility. In other terms, the particle is *dressed* by certain environmental degrees of freedom, and this dressing increases its inertia, or equivalently, its *effective* mass M_{eff}

$$M_{eff} \geq M \equiv M_{free}. \tag{44}$$

This reasoning corresponds to a well understood effect, often observed in scattering from condensed systems; cf. [15, 20, 21]. The last relation holds under the conditions of NCS (DINS) and INS too.

This effect can be also shown by referring to the aforementioned energy conservation relation,

see (42), here including a term $E_{int} > 0$ describing the atom-environment interaction:

$$\bar{E} = \frac{\hbar^2 \bar{K}^2}{2M} + E_{int} \tag{45}$$

where $\bar{E}$ and $\bar{K}$ refer to the center of a peak (measured by a specific detector). Thus there will be a reduced amount of energy, $\bar{E} - E_{int}$, available as kinetic energy to the recoiling particle. As pointed out above, $\bar{E}$ and $\bar{K}$ are determined from the kinematics of the neutron, in contrast to E_{int}, which is a quantity of the scattering system.

Let us now try to fulfill this equation with a pair (E_{IA}, K_{IA}) being determined by the conventional theory in the impulse approximation (IA), for which holds

$$E_{IA} = \frac{\hbar^2 K_{IA}^2}{2M_{eff}} \tag{46}$$

Obviously, from the last two equations follows $M_{eff} > M$.

This effect may be demonstrated with the aid of a DINS result by Sokol et al. [23], obtained from H atoms produced by chemisorbed, dissociated H_2 in the graphite intercalation compound (GIC) C_8K. The experiment was done with a so-called *inverse geometry* TOF spectrometer (of Argone Nat. Lab., USA) with energy selection in the *final* flight path and chosen momentum trasfer with $K = 39$ Å^{-1}, which is high enough for the IA to be valid. Additionally, an accompanying DINS experiment from the ionic solid KH was done with the same instrumental setup. The similarity between the H recoil peaks in KH and the GIC, see Fig. 4, led to the conclusion that the state of H is similar in both samples [23]. The measured position of the H peaks corresponds to a very high effective mass, i.e. $M_{eff} = 1.2$ a.m.u.

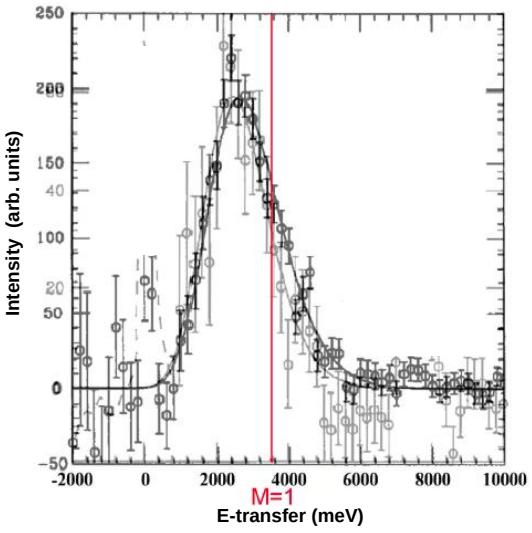

Figure 4. The conventional effect $M_{eff} > M$ — DINS from chemisorbed H in C_8K, adapted from figues of [23]. The maxima of the H peaks are about 2620 meV The vertical red line indicates the position of a $M = 1$ a.m.u. recoil peak (at 3540 meV), assuming that the conventional theory (here: the IA) is obeyed. — Black points and fitted line: KH, Grey points and fitted line: $C_8K_{0.9}H_{0.13}$. The spectra were recorded with a selected final neutron energy E_f =4280 meV. The peak maxima correspond to $M_{eff} = 1.2$ a.m.u.

Thus one obtains the following experimentally testable predictions of conventional theory:

In specifically designed scattering experiments with fixed K-transfer — the so-called *constant-K* measurements — the measured recoil (i.e. kinetic) energy of an atom with mass M will be *smaller* than that predicted by the IA. This is tantamount to a two-body collision of a probe particle (neutron) with a fictitious free atom of mass $M_{eff} > M$.

For more references about FSE and associated discussions of "effective mass" the interested reader may consult Ref. [10].

6. Experiments on the new scattering effect

In this section, the obtained theoretical results are compared with some actually performed experiments. The derivations of the preceding section should apply to all neutron scattering subfields of interest (i.e. INS, NCS, DINS) as the derivations do not contain any specific assumption being valid in one subfield only. The presented experimental results may be considered as examples of the WV-TSVF-theoretical analysis of Section 5.

The revised phyiscal intuitions offered by the theoretical result [8] outlined in Sec. 2 may be understood as the reason that led us to the analysis of the experiments considered here (and several others; see discussion below). In short: The measured scattering signal by a detector is due to a quantum superposition of the neutron

(1) colliding with the atom (and thus giving a "positive" momentum transfer $\hbar K$ to the atom) and

(2) being transmitted without collision, i.e. giving a "zero" momentum transfer,

with the superposition of both causing the atom to receive an additional "negative" component $-\Delta(\hbar K)$ to its total momentum.

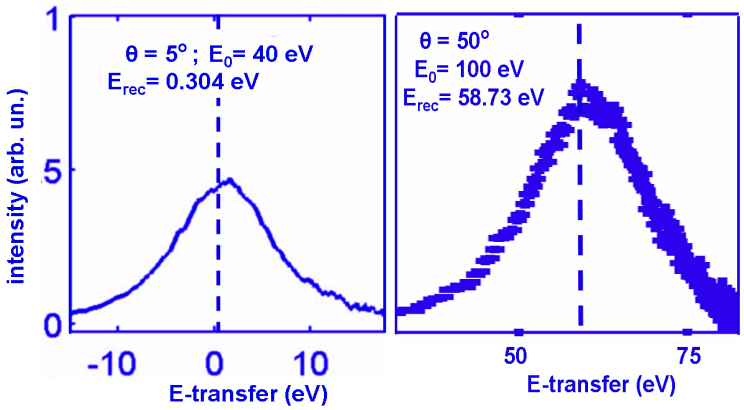

Figure 5. Two examples of DINS spectra from a solid polymer (polyethylene, $[-CH_2-]_n$) measured with the TOF spectrometer MARI of ISIS [24]. Peak-shifts to *higher* energy transfers than the conventionally expected recoil energy E_{rec} (vertical lines) are clearly visible. This effect corresponds to a *lower* effective mass $M_{eff}(\mathrm{H})$ of the recoiling H: $M_{eff}(\mathrm{H}) \approx 0.91 - 0.96$ a.m.u. See [24] for experimental details and more examples.

6.1. NCS/DINS from H atoms of a solid polymer—MARI experiment

An experimental demonstration of the new quantum effect under consideration can be found in the data of [24]. The NCS (or DINS) experiments were carried out by Cowley and collaborators with the TOF spectrometer MARI [25] of the neutron spallation source ISIS (Rutherford Appleton Laboratory, UK). The sample (a foil of a solid polymer, low-density polyethylene) was at room temperature.

Fig. 5 shows two examples of the extensive measurements reported in [24]. The depicted recoil peaks are mainly due to scattering from protons (H atoms), due to the high incoherent scattering cross-section of H [14, 15]. The vertical lines show the E-transfer values according to conventional theory, Eq. (41). The centroids of the measured recoil peaks are markedly shifted to *higher* energy transfer than conventionally expected. As discussed in subsection 5.1, this shift is equivalent to a *smaller* effective mass of the recoiling H atom.

One might object that the shown data contain an additional small contribution from the C recoil. However this is located at smaller E-transfers than that of H, due to their mass difference [15]. Therefore the preceding qualitative conclusion remains unaffected.

It may be noted that the shown NCS peaks are very broad and asymmetric, which is due to the (very) low resolution of the employed modified setup of MARI [24]. This makes a quantitative analysis to determine the peak-position impossible. Nevertheless, visual inspection of the data shows that the centroids of the peaks are *shifted to higher energy* roughly by 5-10 % of the recoil energy, which equivalently means that the effective mass M_{eff} of the recoiling H atoms is *smaller* than $M_H = 1.0079$ a.m.u. of a free H by the same percentage

$$M_{eff}(\mathrm{H}) \approx 0.91 - 0.96 \quad \text{a.m.u.} \tag{47}$$

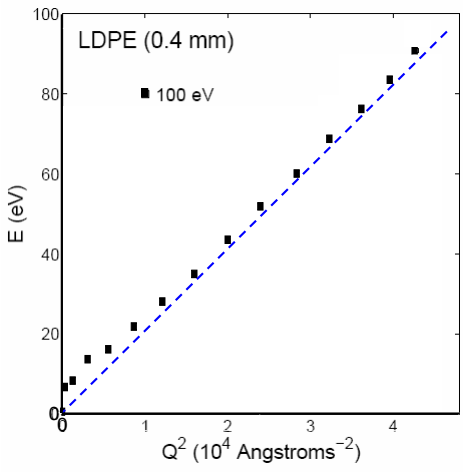

Figure 6. Data from NCS (DINS) from a solid polymer (low-density polyethylene, LDPE), $[-CH_2-]_n$) measured with the TOF spectrometer MARI of ISIS with excitation energy $E_0 = 100$ eV. [24]. The straight line corresponds to the recoil parabola of conventional theory. All data points (center-of-gravity of recoil peaks) show the effect under consideration. i.e. an apparent reduced effective mass of the scattering H-atom. For experimental details and more examples, see [24]. (Data taken from Fig. 12 of [24].)

Throughout this section we presumed that the *calibration* of MARI as employed in the experiment [24] was correct, i.e. that the applied TOF method (see Sec. 5) used correct instrumental parameters.

Moreover, it seems important to look at the additional (about 50) DINS-results being reported in Fig. 12 of Ref. [24], which were obtained at three different excitation energies ($E_i = 20, 40, 100$ eV). Remarkably, *all* those H-recoil peaks — i.e. with no exception! — appeared to show *positive* E-transfers; cf. Fig. 6 which shows data obtained with neutron's initial energy $E_i = 100$ eV. This observation underlines considerably the reliability of the considered "anomalous" E-transfer shift. However, the main aim of that investigation [24] was motivated differently — i.e., the focus was the measurment of the cross-section of H, and to show a weakness of the "inverse geometry" TOF-spectrometer VESUVIO of ISIS — this striking experimental finding remained fully unnoticed and/or uncommented in the discussions of Ref. [24].

6.2. INS from single H_2 molecules in carbon nanotubes

Another surprising result from incoherent inelastic neutron scattering was observed by Olsen et al. [26] in the quantum excitation spectrum of H_2 adsorbed in multi-walled nanoporous carbon (with pore diameter about 8–20 Å).

The INS (or IINS) experiments were carried out at the new generation TOF spectrometer ARCS of Spallation Neutron Source SNS (Oak Ridge Nat. Lab., USA) [11]. In this experiment, the temperature was $T = 23$ K, and the incident neutron energy E_i was 90 meV. The latter implies that the energy transfer cannot excite molecular vibrations (and thus cannot break the molecular bond), but only excite rotation and translation (also called recoil) of H_2 which interacts only weakly with the substrate:

$$E = E_{rot} + E_{trans} \tag{48}$$

The experimental two-dimensional incoherent inelastic neutron scattering intensity map $S(K, E)$ of H (after background subtraction) is shown in Fig. 7, which is taken from the original paper [26]. The following features are clearly visible. First, the intensive peak centered at $E_{rot} \approx 14.7$ meV is due to the well known first rotational excitation $J = 0 \to 1$ of the H_2 molecule [27]. Furthermore, the wave vector transfer of this peak is $K_{rot} \approx 2.7$ Å^{-1}. Thus the peak position in the K–E plane shows that the experimentally determined mass of H that fulfills the relation $E_{rot} = (\hbar K_{rot})^2/2M_H$ is (within experimental error) the mass M_H of the free H atom,

$$\text{rotation:} \quad M_H = 1.0079 \ \text{ a.m.u.} \tag{49}$$

namely, $M_{eff}(H) = M_H$. (a.m.u.: atomic mass units.) In other words, the location of this rotational excitation in the K–E plane agrees with conventional theoretical expectations for IINS, according to which each neutron scatters from a single H [27]. Recall that an agreement with conventional theory was also observed in the case of scattering from ^{4}He [18]; see Fig. 3.

Moreover, the authors provide a detailed analysis of the roto-recoil data from incoherent inelastic neutron scattering, as shown in Fig. 7, and extracted a strongly reduced effective mass of the whole recoiling H_2 molecule (left parabola, green line); see Eq. (41):

$$\text{translation (recoil):} \quad M_{eff}(\mathrm{H_2}) \approx 0.64 \pm 0.07 \ \text{ a.m.u.} \tag{50}$$

This is in blatant contrast to the conventionally expected value $M(\mathrm{H_2}) = 2.01$ a.m.u. for a freely recoiling H_2 molecule (right parabola, red line). (Recall that the neutron-molecule collision does not break the molecular H-H bond.)

An extensive numerical analysis of the data is presented in [26], being based on time-of-flight data analysis (cf. Section 4) and the analysis of the measured data within conventional theory [14, 27].

This strong reduction of effective mass, which is far beyond any conceivable experimental error, corresponds to a strong reduction of momentum transfer by the factor 0.566. Namely, the

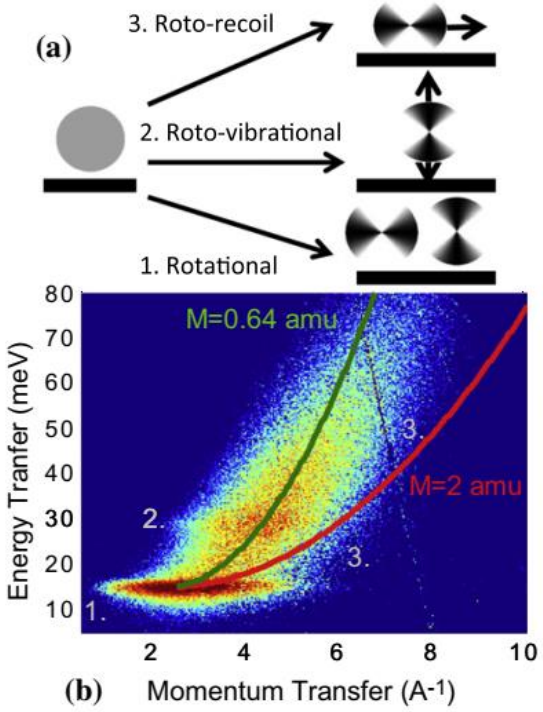

Figure 7. (*a*) Sketch depicting different types of transitions of the hydrogen molecule predicted to be observed by incoherent inelastic neutron scattering (IINS). (*b*) IINS (or INS) intensity map of hydrogen adsorbed in multi-walled carbon nanotubes after background subtraction, with intensity plotted on a log scale. Incident neutron energy is 90 meV and temperature is 23 K. The types of transitions are identified, and a fit to the roto recoil tail is shown (green curve); Fig. 1 of Ref. [26]. — The translation motion of the recoiling H_2 molecules causes the observed continuum of intensity, usually called *roto-recoil* (yellow-orange ribbon), starting at the well visible first rotational excitation of H_2 being centered at $E \approx 14.7$ meV and $K \approx 2.7$ Å^{-1} (red ellipsoid). The K–E position of the latter agrees with conventional theory. In contrast, a detailed fit (green parabola; full line) to the roto-recoil data reveals a strong reduction of the effective mass of recoiling H_2, which appears to be only 0.64 a.m.u. The red curve (on the right) represents the theoretical parabola with the conventionally expected effective mass 2 a.m.u. of a recoiling H_2 molecule. For full details about the data analysis see [26]. (Reproduced from Ref. [26], Fig. 1, with permission from Elsevier.)

observed momentum transfer deficit is about -43% of the conventionally expected momentum transfer. This provides first experimental evidence of the new *anomalous* effect of momentum-transfer deficit in an elementary neutron collision with a recoiling molecule.

Recall that, as explained above (see Subsec. 5.1), every H_2-substrate conventional binding must increase the molecule's effective mass. Thus these findings from IINS are in clear contrast to every conventional (classical or quantum) theoretical expectation. However, they have a natural (albeit qualitative, at present) interpretation in the frame of modern theory of WV and TSVF.

Incidentally, it may be noted that the same *calibration* of ARCS was used in both experiments [18] and [26].

Let us now make a comparison with a related 1-*dimensional* experiment, which may shed more light into the observations under consideration.

The above experimental results also show that the two-dimensional spectroscopic technique, as offered by the advanced TOF-spectrometer ARCS, represents a powerful method that provides novel insights into quantum dynamics of molecules and condensed matter. Clearly, this is due to the fact that K and E transfers can be measured over a broad region of the K–E plane. This advantage makes these new instruments superior to the common one-dimensional ones (like TOSCA at ISIS spallation source, UK), in which the detectors can only measure along a single specific trajectory in the K–E plane. (TOSCA measures along two such trajectories [29].)

As an example, consider the results of [28] from molecular H_2 adsorbed in single-wall carbon nanotubes (which is similar to the material of [26]) at $T \approx 20$ K, as investigated with TOSCA. Also this paper reports the measurement of the roto-recoil spectrum, but as a function of E only (due to the aforementioned single trajectory in the K–E plane being instrumentally accessible). Therefore for the theoretical analysis of the data the mass of H_2 was *fixed* to its conventionally expected value of 2 a.m.u., and thus the strong anomalous effect, Eq. (50), remained unnoticed; see [28], p. 903.

7. Discussion

Due to the novelty of the theory of WV and TSVF, several counter-intuitive features therein and in its applications may appear "strange" or even "wrong". Aiming to clarify some of them, here we provide additional remarks and explanations.

(A) *Instrumental calibration* — The results presented above have considerable consequences for the calibration of the associated TOF spectrometers. In particular, in NCS (DINS) instrumentation, it is a common practice to use the recoil peaks of light atoms (typically H, D or He) to achieve an "optimal" calibration of the spectrometer. In other words, the measured positions of a peak in the K–E plane — together with the standard free-atom recoil expression of Eq. (41), sometimes also improved with FSE — are used in order to "fine tune" the numerical values of the instrument's parameters determining the measured TOF values. Obviously, such a "optimization" of the calibration leads automatically to an artificial agreement of the data with conventional theory.

(B) Note that in in our approach, the two operators $\hat{q}$ and $\hat{P}$ occurring in the von Neumann-type interaction Hamiltonian of Eq. (25) refer to two *different* quantum systems. Thus, according to Vaidman [30], the concept of WV arises here due to the interference of a quantum *entangled* wave and therefore it has no analog in classical wave interference. This further supports the conclusion that WV is a genuinely quantum concept and not some kind of "approximation".

In contrast, conventional neutron scattering theory treats the neutron as a classical mass point. Namely, consider the basic formulas of the theory, e.g. the expression for the partial differential cross-section

$$\frac{d^2\sigma_A}{d\Omega d\omega} = \frac{k_f}{k_i} b_A^2 S(\mathbf{K}, \omega) \tag{51}$$

($E = \hbar\omega$, $d\Omega$: solid angle measured/covered by the detector.) $S(\mathbf{K}, \omega)$ is the dynamic structure factor of the scattering system, which contains degrees-of-freedom of the scattering particles only. This equation contains *no dynamical* variable of the neutron at all — the neutron is "degraded" to a classical object and only its scattering length b_A — a c-number capturing its scattering properties from atom A — appears here. This fact is a specific feature of the first Born approximation and/or first-order perturbation theory which the conventional theory is based on [14, 15].

(*C*) The momentum-transfer deficit, and the associated effective-mass reduction of the scattering particle A, may appear to someone as violating the energy and momentum conservation laws of basic physics. However, this is not the case, because the scatterer A is *not* an isolated, but an *open* quantum system. Thus we may say that the quantum dynamics of the "environment" of A, which participates to the neutron-A scattering, is indispensable for the new WV-TSVF effect under consideration. Thus it may be helpful to write down the "conservation" relations

$$E_{H+env} = -E_n \quad \text{and} \quad \hbar K_{H+env} = -\hbar K_n \tag{52}$$

which express energy and momentum conservation for the case that the *environment* (indicated with the subscript *"env"*) of the scattering H is not neglected. The theoretically derived momentum transfer deficit, when interpreted (or better: misinterpreted) in terms of conventional theory, is equivalent to scattering of a neutron from a ficticious particle representing the *whole* H+environment system, which has a mass M_{eff} being smaller than the mass of a free H-atom — or, in other terms, the environment of H seems to have a negative mass!

(*D*) The INS results from H_2 in C-nanotubes [26] discussed in subsection 6.2 appear contradictory — in the frame of conventional theory — because of the following two main points:

(*i*) The observed $J = 0 \rightarrow 1$ rotational excitation of the H_2 molecule by the collision with a neutron exhibits a $M_{eff} \approx 1$ a.m.u., see Eq. (49), as conventionally expected. Namely, the scattering is incoherent, i.e. the neutron exchanges energy and momentum with one H only.

(*ii*) In contrast, in the same experiment, the M_{eff} of the observed roto-recoil response of the whole H_2 molecule is not 2 a.m.u. as it should (because the whole H_2 undergoes a translational motion), but only $M_{eff} \approx 0.64$ a.m.u., see Eq. (50).

However, this "contradiction" just disappears in the light of the new theory, because it simply implies that the quantum *environment* of H in case (*i*) must be *different* from that in case (*ii*) — the locally rotating H_2 is much less influenced by its environmental interactions than the translating H_2, which necessarily interacts with a greater environmental part during its translational motion caused by its collision with the neutron.

(*E*) In the scientific literature one often meets the criticism that *post-selection* just means "throwing out some data". In the experimental context at issue, however, post-selection certainly means "performing a concrete measurement on the system, using a well defined detector, and analyzing the measured data only". In this context it may be helpful to mention the paper by Wu [31], in which he offers a slight extension of the WV and TSVF that does not discard any data. Furthermore, it is shown how the matrix elements of any generalized state (pure or mixed) can be directly read from appropriate weak measurements.

(*F*) Concerning the applicability of WV (and WM) to the neutron scattering process, one may object that the neutron-nucleus potential (i.e., the conventional Fermi pseudopotential [14]) may be not "weak" in the specific sense of the new theory. Therefore it is helpful to mention the recent generalization of the considered WM and WV theory by Oreshkov and Brun [32]. The authors showed that WM are universal, in the sense that any generalized measurement can be decomposed into a sequence of WMs. This important theoretical result is further supported by the work of Qin et al. [33], who showed that the main WM results can be extended to the realm of *arbitrary* measurement strength.

(*G*) Very recently, some qualitatively new theoretical results of WV-TSVF have been obtained, a few of which should be mentioned here:

(a) The quantum Cheshire-Cat effect [34], which has also been observed experimentally [35].
(b) The predicted quantum violation of the Pigeonhole principle [36].

These new results point once more to a very interesting structure of quantum mechanics that was hitherto unnoticed. Moreover, they also shed new light on the very notions of separability, quantum correlations and quantum entanglement [37].

(H) The exploration of the "anomalous" momentum exchange taking place on a mirror of a MZI [8], as discussed in Sec. 2, indicates that this effect could also be relevant in the context of the widely applied methods of small-angle neutron scattering (SANS), small-angle X-ray scattering (SAXS) and reflectometry on surfaces and/or thin multilayer structures of physico-chemical and biological materials.

(I) Recently, quantum interference and entanglement [37] effects have been recognized to be crucial for quantum computing and quantum information theory; cf. [38]. Hence it seems interesting to explore the potential applicability of the new quantum features connected with WV, TSVF and the momentum transfer deficit (or energy transfer surplus) to recently emerging fields of quantum computational complexity theory [39, 40], and/or ICT (information and communication technology).

(J) In view of the experimentally detected effects of Sec. 6, and in particular of the striking reduction of effective mass due to quantum interference, it seems appropriate to mention here some speculative ideas concerning a possible *practical* and/or *technological* importance of the new theory. Namely:

(1) a more mobile (i.e. with smaller effective mass) H atom (or H^+ ion) in a properly designed fuel cell material would facilitate proton transfer and thus also increase the efficiency of the fuel cell;

(2) a properly designed solid environment (or nanostructure) of Li^+ ions in a Li-ion-battery would result in a lower Li^+ effective mass, thus allowing a faster ionic mobility and a *faster recharging* process — with obvious advantages for current technological efforts.

Concluding, the present author believes that the theoretical formalism of WM, WV, and TSVF not only sheds new light on interpretational issues concerning fundamental quantum theory (like e.g. the time-inversion invariance of the basic physical laws, the meaning of quantum entanglement and correlations, etc.) but it also offers a fascinating new guide for our intuition to predict new effects, and also helps to plan and carry out new experiments and reveal novel quantum phenomena.

Acknowledgments
I wish to thank Erik B. Karlsson (Uppsala) and Ingmari Tietje (CERN) for helpful discussions, and COST Action MP1403 – Nanoscale Quantum Optics – for partial financial support.

[1] Aharonov Y and Rohrlich D 2005 *Quantum Paradoxes: Quantum Theory for the Perplexed* (Weinheim: Wiley-VCH)
[2] Aharonov Y, Albert D Z and Vaidman L 1988 *Phys. Rev. Lett.* **60** 1351
[3] Aharonov Y and Vaidman L 1990 *Phys. Rev. A* **41** 11
[4] Kofman A G, Ashhab S and Nori F 2012 *Phys. Rep.* **520** 43
[5] Tamir B and Cohen E 2013 *Quanta* 2013; **2** 7
[6] Aharonov Y, Cohen E and Elitzur A C 2014 *Phys. Rev. A* **89** 052105
[7] Dressel J, Malik M, Miatto F M, Jordan A N and Boyd R W 2014 *Rev. Mod. Phys.* **86** 307
[8] Aharonov Y, Botero A, Nussinov S, Popescu S, Tollaksen J and Vaidman L 2013 *New J. Phys.* **15** 093006
[9] Aharonov Y, Bergmann P G and Lebowitz J L 1964 *Phys. Rev.* **134**, B1410
[10] Chatzidimitriou-Dreismann C A 2016 *Quanta* **5** 61-84

[11] https://neutrons.ornl.gov/ARCS
[12] Scully M O and Zubairy M S 1997 *Quantum Optics* (Cambridge: Cambridge University Press)
[13] von Neumann J 1932 *Mathematische Grundlagen der Quantenmechanik* (Berlin: Springer Verlag) [English translation: 1955 *Mathematical Foundations of Quantum Mechanics* (Princeton: Princeton University Press]
[14] Squires G L 1996 *Introduction to the Theory of Thermal Neutron Scattering* (Mineola: Dover)
[15] Watson G I 1996 *J. Phys.: Condens. Matter* **8** 5955
[16] Aharonov Y, Cohen E and Ben-Moshe S 2014 *EPJ Web of Conferences* **70**, 00053
[17] Feynman R P, Leighton R B and Sands M 1965 *The Feynman Lectures on Physics, Vol. III, Quantum Mechanics* (Reading: Addison-Wesley Publ.) [Also available at: http://www.feynmanlectures.caltech.edu/]
[18] Diallo S O, Azuah R T, Abernathy D L, Rota R, Boronat J and Glyde H R 2012 *Phys. Rev. B* **85** 140505
[19] Feynman R P, Leighton R B and Sands M 1965 *The Feynman Lectures on Physics, Vol. I* (Reading: Addison-Wesley Publ.)
[20] Tietje I C 2012 *J. Phys.: Conf. Ser.* **380** 012014
[21] Sears V F 1984 *Phys. Rev. B* **30** 44
[22] Hohenberg P C and Platzman P M 1966 *Phys. Rev.* **152** 198
[23] Schirato B S, Herwig K W, Sokol P E and White J W 1990 *Chem. Phys. Lett.* **165** 453
[24] Stock C, Cowley R A, Taylor J W amd Bennington S M 2010 *Phys. Rev. B* **81** 024303
[25] Science and Technology Facilities Council, ISIS facility, Oxfordshire, UK, spectrometer MARI. (http://www.isis.stfc.ac.uk/instruments/MARI/)
[26] Olsen R J, Beckner M, Stone M B, Pfeifer P, Wexler C and Taub H 2013 *Carbon* **58** 46
[27] Mitchell P C H, Parker S F, Ramirez-Cuesta A J and Tomkinson J 2005 *Vibrational Spectroscopy with Neutrons.* (New Jersey: World Scientific)
[28] Georgiev P A, Ross D K, De Monte A, Montaretto-Marullo U, Edwards R A H, Ramirez-Cuesta A J, Adams M A and Colognesi D 2005 *Carbon* **43** 895
[29] http://www.isis.stfc.ac.uk/instruments/TOSCA/
[30] Vaidman L 2014 *Comment on "How the result of a single coin toss can turn out to be 100 heads"* arXiv:1409.5386 [quant-ph].
[31] Wu S 2013 *Sci. Rep.* **3** 1193
[32] Oreshkov O and Brun T A 2005 *Phys. Rev. Lett.* **95** 110409
[33] Qin L, Feng W and Li X-Q 2016 *Sci. Rep.* **6** 20286
[34] Aharonov Y, Popescu S and Skrzypczyk P 2013 *New J. Phys.* **15** 113015
[35] Denkmayr T, Geppert H, Sponar S, Lemmel H, Matzkin A, Tollaksen J and Hasegawa Y 2014 *Nat. Commun.* **5** 4492
[36] Aharono Y, Colombo F, Popescu S, Sabadini I, Struppa D C and Tollaksen J 2016 *Proc. Nat. Acad. Sci. USA* **113** 532
[37] Horodecki R, Horodecki P, Horodecki M and Horodecki K 2009 *Rev. Mod. Phys.* **81** 865
[38] Nielsen M A and Chuang I L 2000 *Quantum Computation and Quantum Information* (Cambridge: Cambridge University Press)
[39] Arora S and Barak B 2009 *Computational Complexity – A Modern Approach* (Cambridge: Cambridge University Press)
[40] Fortnow L 2009 *Communications of the ACM* **52** 78